Fall 12-2020

Novel Computational Infant Musculoskeletal Model for Biomechanical Analysis of Infant Movement

Yeram Lim
Embry-Riddle Aeronautical University

NOVEL COMPUTATIONAL INFANT MUSCULOSKELETAL MODEL FOR BIOMECHANICAL ANALYSIS OF INFANT MOVEMENT

by

Yeram Lim

A Thesis Submitted to the College of Engineering Department of Mechanical Engineering in Partial Fulfillment of the Requirements for the Degree of Master of Science in Mechanical Engineering

Embry-Riddle Aeronautical University
Daytona Beach, Florida
December 2020

NOVEL COMPUTATIONAL INFANT MUSCULOSKELETAL MODEL FOR BIOMECHANICAL ANALYSIS OF INFANT MOVEMENT

by

Yeram Lim

This thesis was prepared under the direction of the candidate's Thesis Committee Chair, Dr. Victor Huayamave, Assistant Professor, Daytona Beach Campus, and Thesis Committee Members Dr. Christine Walck, Assistant Professor, Daytona Beach Campus, and Dr. Alesha Fleming, Assistant Professor, Daytona Beach Campus, and has been approved by the Thesis Committee. It was submitted to the Department of Mechanical Engineering in partial fulfillment of the requirements for the degree of Master of Science in Mechanical Engineering

Thesis Review Committee:

V Huayamave
Victor Huayamave, Ph.D.
Committee Chair

Christine D Walck
Christine Walck, Ph.D.
Committee Member

Alesha Fleming, D.C.
Alesha Fleming, D.C.
Committee Member

Jean michel Dhainaut
Jean-Michel Dhainaut, Ph.D.
Graduate Program Coordinator,
Mechanical Engineering

Eduardo Divo
Eduardo. Divo, Ph.D.
Department Chair,
Mechanical Engineering

Maj Dean Mirmirani
Maj Mirmirani, Ph.D.
Dean, College of Engineering

Christopher Grant
Christopher Grant, Ph.D.
Associate Vice President of Academics

11/30/2020
Date

Acknowledgements

I would like to acknowledge the faculty and staff of Embry-Riddle Aeronautical University, specifically the members of the committee: Dr. Victor Huayamave (Committee chair), Dr. Christine Walck (Committee member) and Dr. Alesha Fleming (Committee member) for pushing me, guiding me, and always being available to help throughout this study. I would also like to thank my family and friends; without their prayers and support, I would not have made it this far. I also thank Dr. Erin Mannen and Dr. Safeer Siddicky of Boise State for their advising, and collaboration for this study.

Abstract

Researcher: Yeram Lim

Title: Novel Computational Infant Musculoskeletal Model for Biomechanical Analysis of Infant Movement

Institution: Embry-Riddle Aeronautical University

Degree: Master of Science in Mechanical Engineering

Year: 2020

Computational musculoskeletal models are increasing in commonality and popularity in the study of biomechanics. These models, however, are mainly used to represent fully developed adults, while infant musculoskeletal models are nonexistent. This study aims to develop a novel computational infant musculoskeletal model for biomechanical analysis of infant movement. For this study, 31 reflective markers were placed on an infant, and marker-based motion capture data was collected. The computational study used a generic GAIT2392 OpenSim musculoskeletal model that was scaled to create a customized subject-specific infant model. By using the motion capture data recorded of the infant during a kicking motion, and a constant ground reaction force value of 52.48 N to represent the infant's weight, the hip joint angle and external joint moment was calculated using inverse kinematics and inverse dynamics. Preliminary results showed a hip joint angle starting at 23.4° and 33.8° at the beginning of a kick, which then flexes to 66.6º and 66.3º at peak hip flexion, and then decreases to 40.2° and 39.9º in the right and left hip joint, respectively. A external hip joint moment of 0.81 N*m and 0.96 N*m was observed at the beginning of the kick, which then decreased to 0.27 N*m and 0.037 N*m at peak him flexion, and the increased to 0.49 N*m and 0.76 N*m at the end of the kick in the right and left hip joint, respectively. These results compare to results found in

literature. A difference of 30.5 and 30.8 was observed in the right and left hip joint at the point of peak hip flexion, respectively, and a difference of 0.28 N*m and 0.083 N*m was observed in the right and left external hip joint moment at the point of peak hip flexion, respectively. Although these values are different, a decrease in external hip joint moment is observed as the hip is flexed, which then increases as the hip joint is extended, which correlates to the trend found in literature. From these results, it was concluded the infant musculoskeletal model will properly portray the biomechanics behind infant movement and can quantify the joint angle and external joint moments to further study the effect of pathologies in infants.

Table of Contents

List of Tables

Page

List of Figures

Page

Chapter I

Introduction

The human movement is a complex combination requiring both neurological and musculoskeletal involvement. By studying these movements, a normal characterization can be determined for specific movements. These normative characteristics are used in the comparison of movements seen in subjects who are affected by previous injuries or pre-existing pathologies. Musculoskeletal modeling is used to replicate these common human movements, allowing for the computation and quantification of kinematics, kinetics, and muscle activity using marker-based motion capture, force plates, and electromyography sensors. Musculoskeletal computational modeling is a non-invasive method of observing biomechanical responses during movements that are difficult to observe using traditional experiments. By taking the measurements of the subject's body segments, such as torso, femur, and tibia, a physiologically accurate subject-specific model can be created. The ability to create a subject-specific model allows for the simulated dynamic movements to be recreated to accurately represent real-life movements.

The use of musculoskeletal computational modeling has advanced exponentially in the study of biomechanics. This method is observed being used in the study of biomechanical responses in sports performance [1], clinical outcomes [2, 3, 4, 5], occupational ergonomics [6, 7], and accident reconstruction [8]. Although there have been rapid advancements on musculoskeletal computational modeling, most of these advancements have been made on adult human musculoskeletal modeling, while neonatal and infant populations are under-represented.

Infant musculoskeletal computational models are uncommon due to the lack of experimental data. The limited subject pool of infant subjects, and lack of control in conducting regulated movements needed to observe the normative characteristics during these movements makes the data needed scarce. The phases of infant development of learning motor control and coordination is a vital stage of development where the anatomy and neuromuscular and sensory systems undergo rapid changes [9], making the development of a valid subject-specific musculoskeletal computational model of an infant a crucial step to a better understanding infant growth and development, and observed movements. Several pathologies, including cerebral palsy (CP) and developmental dysplasia of the hip (DDH), that can be detected during the early stages of infancy using the musculoskeletal modeling technique can help with early interventions during infancy [10], improve access to community services [11], and improve the overall well-being for parents [12]. Subject-specific computational models most accurately represent physiological movements. However, the development of infant subject-specific musculoskeletal computational models is a multi-step process requiring anthropometric measurements, 3D kinematic data using motion capture, and kinetic data using force plates.

The purpose of this work is to develop a preliminary single subject infant computational model using OpenSim, using anthropometric measurements from experimental motion capture data of a single infant to further study the physiological movements of infants. Specifically, the movements observed in the hip will be studied and compared to previous literature to create a preliminary model able to observe healthy

infant hip movements to better quantify the movements seen in infants with developmental dysplasia of the hip.

Chapter II

Review of the Relevant Literature

2.1 Musculoskeletal Computational Modeling

For this study, OpenSim, a three-dimensional musculoskeletal modeling software, was used to create the musculoskeletal computational model. OpenSim is an open-source software project developed at Stanford University that allows researchers to access, modify, and develop different musculoskeletal models to conduct research. These models have been used in a wide variety of research applications, such as biomechanics, medical device design, orthopedics, sports science, and robotics research. An OpenSim model is made up of several parts, the main ones being bodies, joints, forces, and markers.

The body of an OpenSim model are rigid segments that represent the skeletal bone structure of an anatomical human. These rigid segments are connected by joints that represent joints seen in the human body, such as the knee joint and ankle joint. These joints allow the bodies to move with respect to each other. On the bodies are muscles represented by lines segment, with the respective origin and insertion points. An insertion point of a muscle is the point on the body or bone the muscle is attached to moves during the motion, while the origin point of a muscle is the point on the body or bone the muscle is attached to remains immobile. These muscles also represent one of the force elements in the model, the other being external forces obtained through force plates. These muscle forces are characterized by muscle parameters in OpenSim, such as maximum isometric force, optimal fiber length, tendon slack length, and pennation angle. On each model, there are virtual markers connected to the bodies, as opposed to experimental markers obtained from kinematic data.

2.1.1 OpenSim GAIT2392

For this study, the OpenSim model GAIT 2392 (Figure 1) was used. The GAIT 2392 model is a model consisting of muscles in the lower extremity [13].

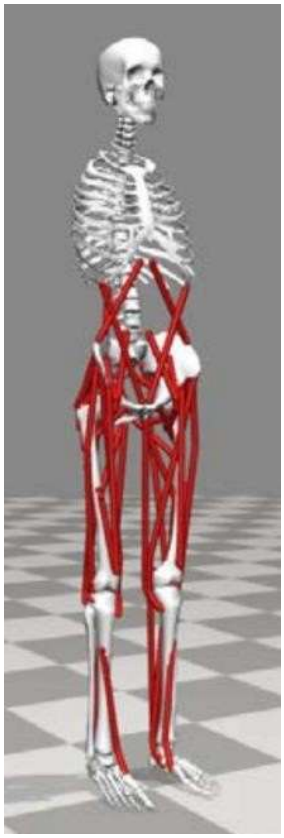

Figure 1. OpenSim Gait 2392 Model

The GAIT 2392 model has a 23 degree of freedom and 96 musculotendon actuators that represent 76 muscles in the lower extremity, including pelvis, femur, tibia, fibula, talus, foot, and toes, designed and mainly used for the simulation of leg dominant motions. The GAIT 2392 model was used due to its representation of the lower extremity while excluding any complexity of the upper extremity movements. This model, along with all the other models used on OpenSim, utilizes the Hill model in order to accurately portray muscle performance. The Hill model uses three

components to predict the active and passive muscle forces: contractile element, parallel elastic element, and serial elastic element [14]. According to Seow (2013), the contractile element (CE) predicts active muscle forces and specific muscle characteristics, the parallel elastic (PE) element predicts the elastic structures covering the muscles as well as the passive muscle forces, while the serial elastic (SE) element predicts the tendon forces which equal the summation of the contractile and parallel elastic element forces (Figure 2).

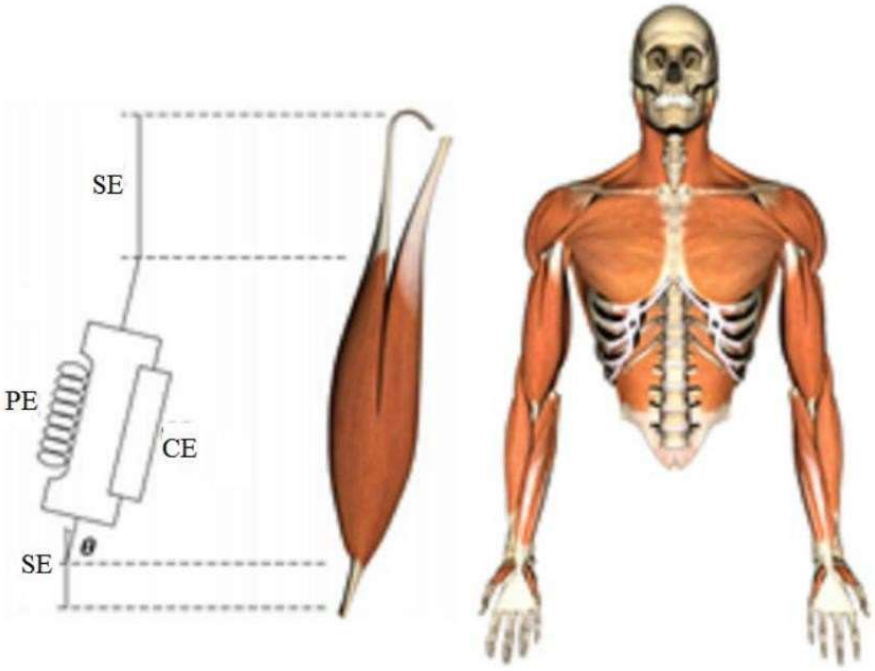

Figure 2. Hill Model used in OpenSim models. CE predicts active muscle forces, PE predicts elastic and passive muscle force, and SE predicts the overall summation of CE and PE forces.

2.2 The Hip Joint

2.2.1 Anatomy

There are three planes of motion that pass through the human body: coronal (frontal) plane, transverse (horizontal) plane, and the sagittal plane. The sagittal plane lies vertically, diving the body into left and right parts. The coronal or frontal plane also lies vertically, dividing the body into anterior and posterior parts. The transverse or horizontal plane lies horizontally, diving the body into superior and inferior parts. (Figure 3).

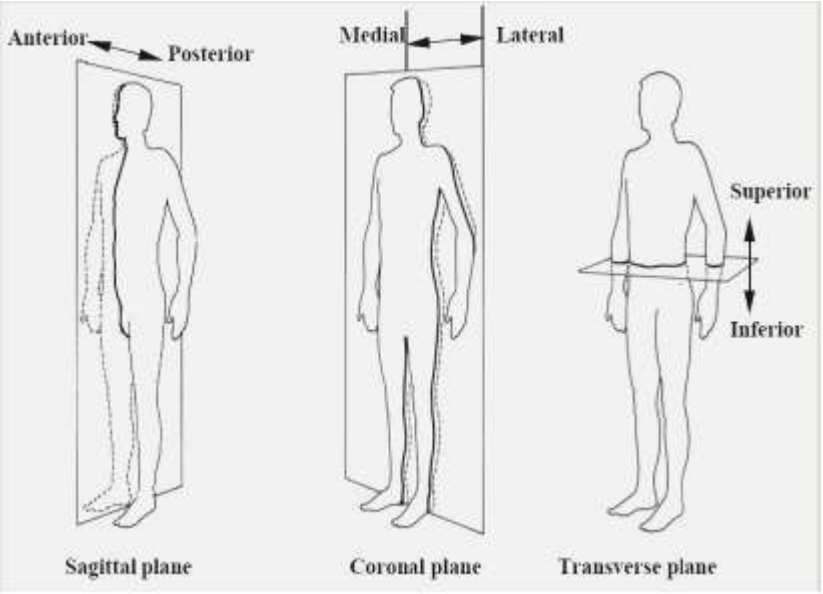

Figure 3. Plane of movements: sagittal, coronal, and transverse planes [2].

The anatomy of the hip joint consists of the femoral head and the acetabulum (Figure 4).

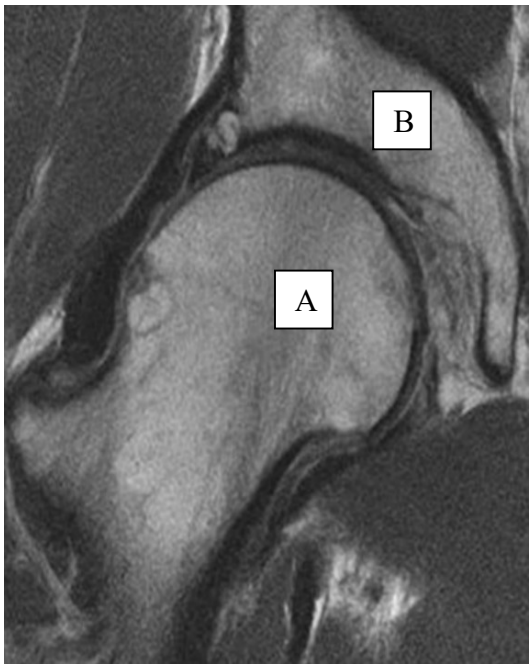

Figure 4. Anatomy of the hip joint: A. Femoral Head and B. Acetabulum.

At birth, the hip joint is made of soft cartilage that slowly ossifies over time into bone. The hip joint can be categorized as a ball-and-socket joint, the femoral head being the ball and the acetabulum being the socket. If the infant in the womb is crowded, the femoral head can be pushed out of place, causing the developing hip joint to become shallow, causing developmental dysplasia of the hip (DDH).

2.2.2 Developmental Dysplasia of the Hip

DDH is a disorder commonly diagnosed as a childhood disability. DDH is an underlying cause for up to 9% of all primary hip replacements and up to 29% of those seen in people aged 60 years and younger [15]. Studies have also shown that there are about 20 cases of some instability per 1000 births [16], and 6 out of 1000 cases will require treatment [17].

The previous method of diagnosing DDH has been the Ortolani and Barlow method. The Ortolani method consists of the flexed hip being abducted, and a gentle anterior force being applied, while the Barlow method consists of the flexed hip being abducted, and a posterior force applied.

In both cases, an audible sound can be heard if the hip joint is dislocated. Contrary to the Ortolani and Barlow method, the classification method used by the IHDI is a radiographic classification system that uses the midpoint of the proximal femoral metaphysis as a reference landmark [18]. There are four grades of dislocation related to DDH, Grade 4 being the most severe (Figure 5) as specified by the International Hip Dysplasia Institute (IHDI) [18].

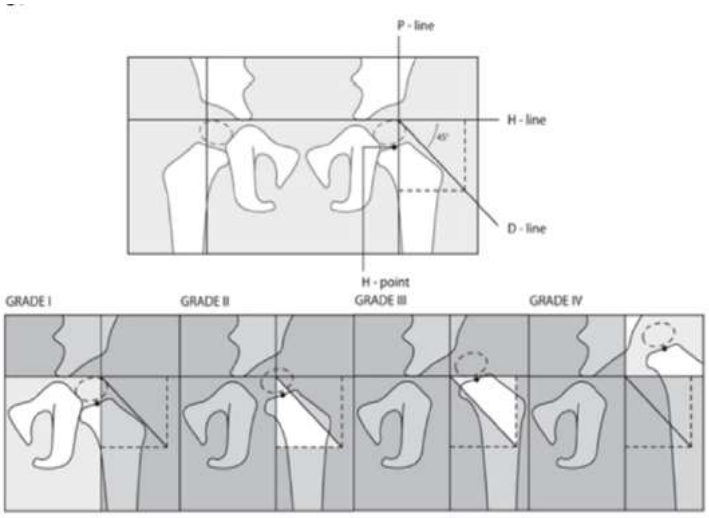

Figure 5. Classification of developmental dysplasia of the hip. Grade 1 being the mildest and Grade 4 being the most extreme. Grade I: The H-point is medial to the P-line. Grade II: The H-point is lateral to the P-line and at/medial to the D-line. Grade III: The H-point is lateral to the D-line and at/inferior to the H-line. Grade IV: The H-point is superior to the H-line.

Due to the dislocation of the femoral head and the change of subsequent muscle moment arms, it is the hypothesis that the biomechanical response observed in a dysplastic hip will differ than that of a healthy hip.

2.2.3 Infant Movement

During the newborn stage of infants, they can be considered immobile, all their movements appear to be jerky, and random in nature. These spontaneous and random movements can be categorized as more of reflexes rather than voluntary movements. After a year of development, however, the movements observed are more controlled, with purpose, and smooth. This developmental change can be accounted for by the maturation of the central nervous system (CNS) [19].

Joint movements are often created through the activation of these muscles through rotational forces or torques. The rotation at the hip joint during a soccer kick is an example of such an outcome. The movement of the thigh, leg, foot, and various muscles around the hip all cause the rotational movement of the hip seen in a soccer kick. A hip joint moment rotation is also observed during the spontaneous movements of the lower extremity in infants.

In a study conducted in 1990 by Schneider et al., the purpose was to quantify the kinematics and kinetics of the hip joint during an infant's kick. Anthropometric data of 6 infants at an average age of 3.1 ± 0.48 months old and total body mass of 6.13 ± 0.61 kg. The upper extremity of the subject during the trial was strapped down using a strap wrapped around the subject's chest and abdomen to stabilize the upper extremity, as well as reduce upper body movement (Figure 6).

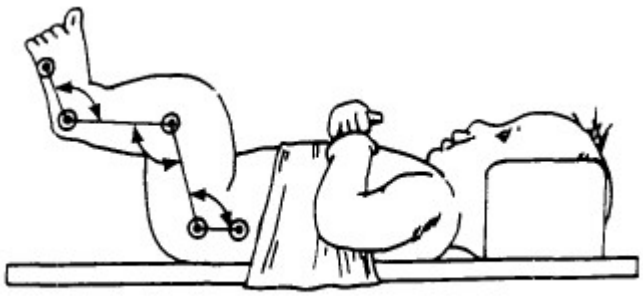

Figure 6. Experimental set up of Schneider et al.: Infant in supine position with upper extremity strapped [19].

A kick was defined as a movement of the lower limb, beginning at an extended position, moving through an entire hip flexion phase, and then returning to the extended position. The kick analyzed was of medium intensity, comparative to other kicks that was recorded, and was a single kick of 0.8 seconds taken from a series of kicks. This kick was recorded using infrared light-emitting diodes, detected by infrared-sensitive cameras to collect kinematic data, and calculate the joint angles of the hip during the kick motion (Figure 7).

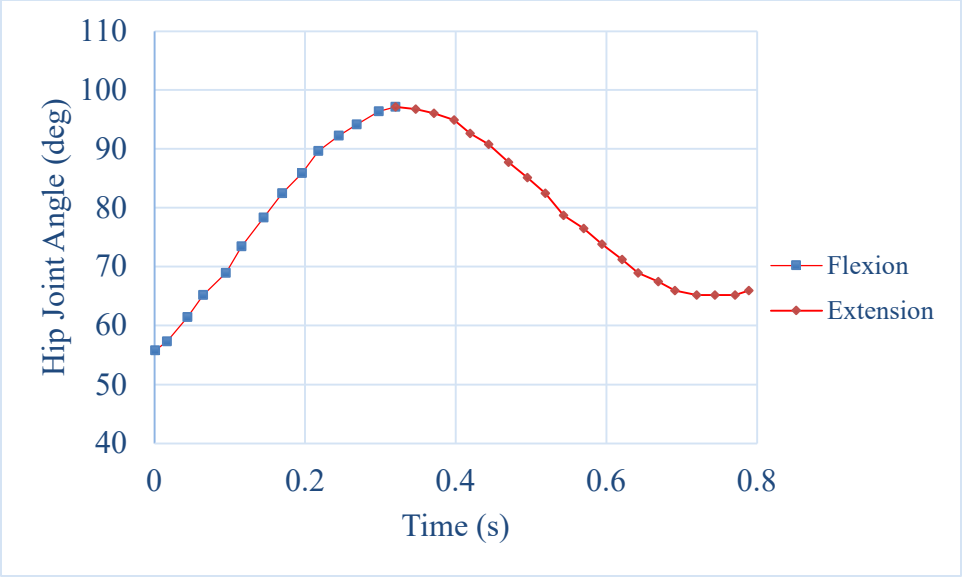

Figure 7. Characteristic patterns of the hip during kicking: time series for the hip joint angles [19].

In order to calculate the net joint torque seen in the hip joint (Figure 8), the inverse dynamics approach was used.

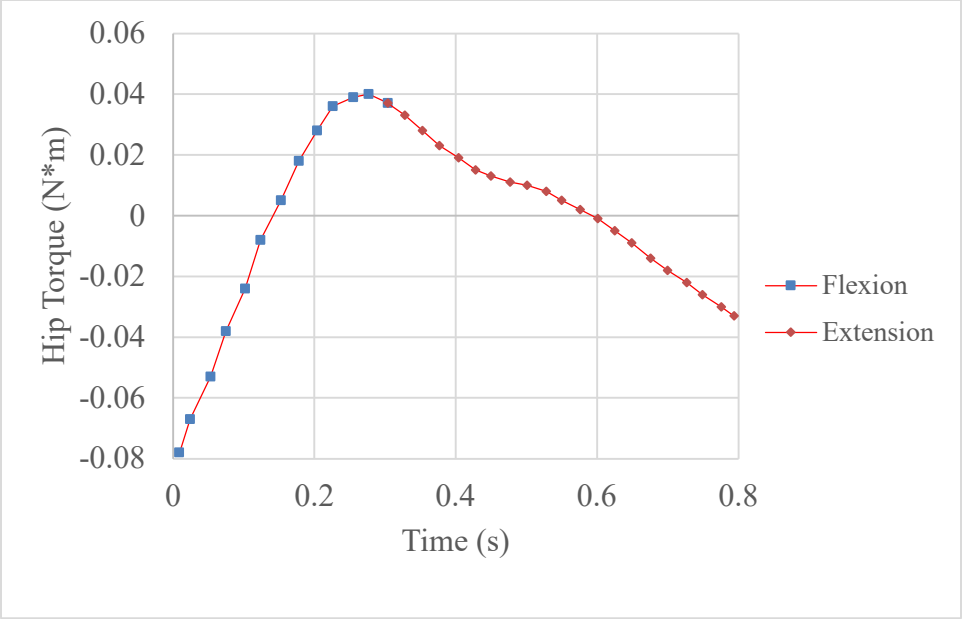

Figure 8. Characteristic patterns of the hip joint movements during kicking: net joint torque at the hip [19].

By knowing the segmental masses, center-of-mass locations, and moments of inertia, the torques were calculated about the axes normal to the moving plane passing through the joints. The net joint calculated included the gravitational torques, interactive torques, and generalized muscle torques. The gravitational torques cover the passive torque resulting from gravity acting on the center of mass of each moving segment. The interactive torques cover the passive, motion dependent torques from mechanical interactions between segments. The generalized muscle torques cover the forces from active muscle contractions and passive deformations of muscles. Schneider et al. (1990) calculated the net hip joint torque as a sum of three torques: 1. Gravitational torque: torque resulting from gravity acting at the center of mass of each segment, 2. Interactive torque(s): torque(s) resulting from motion-dependent torques resulting from the motion of the segments and ground reaction forces, and 3. Generalized muscle torque: generalized

torques that include forces from active and passive muscle, tendons, ligaments, and other tissue contractions. OpenSim's inverse dynamics tool calculates the external joint torque using two of the three used in Schneider et al. (1990)'s study: gravitational torque and interactive torques. The hip joint torque graph from Schneider et al. (1990)'s study was modified to represent the two torques seen in OpenSim's inverse dynamics calculations for comparison (Figure 9).

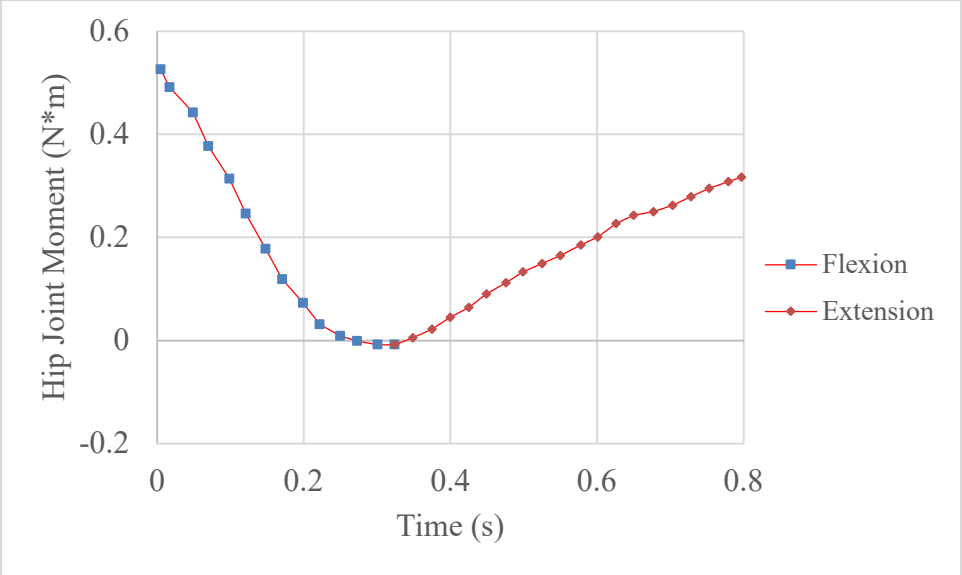

Figure 9. Hip joint moment plot representing gravitational and interactive torque values [19].

Chapter III

Methodology

To investigate the biomechanical responses of the hip joint during an infant's spontaneous kicking, the following pipeline was followed throughout the study (Figure 10).

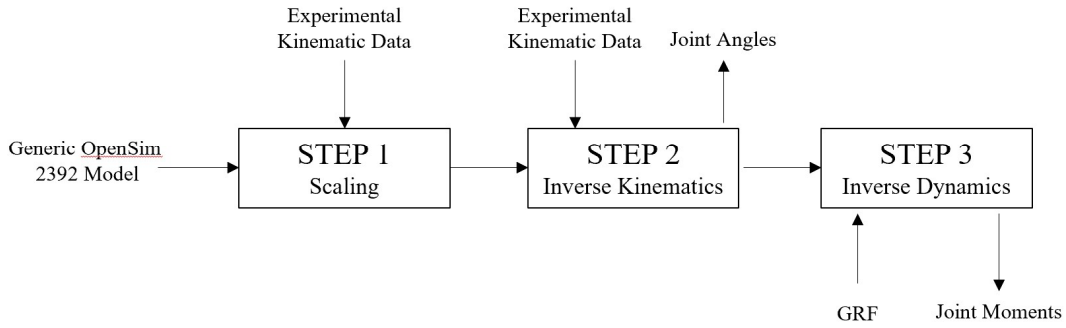

Figure 10. Pipeline followed on OpenSim.

3.1 Scaling

Three-dimensional motion capture data was collected at the University of Arkansas Medical Center, used to drive a subject-specific musculoskeletal model developed within OpenSim (Figure 11).

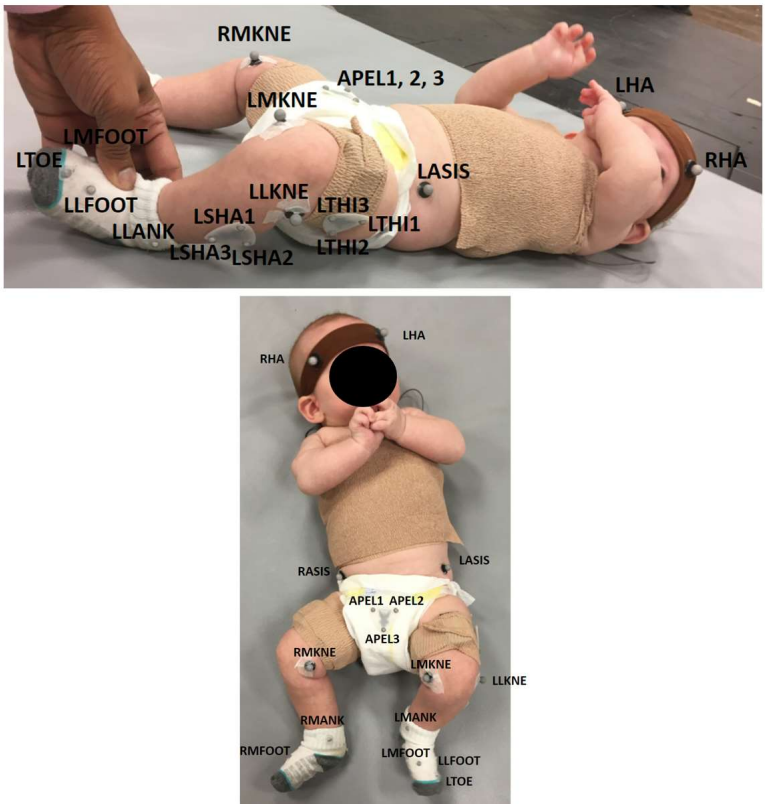

Figure 11. Infant subject with experimental marker placements

Marker-based motion capture (100 Hz; Vicon, Oxford, UK) recorded movement through reflective markers placed bilaterally on the anterior and posterior of the head, anterior superior iliac spine (ASIS), posterior superior iliac spine (PSIS), greater trochanter, medial and lateral epicondyles of the knee, and the medial and lateral malleolus of the ankle. Additionally, three-marker clusters were placed on the anterior and posterior of the pelvis, and bilaterally on the lateral aspect of each thigh.

The scale tool within OpenSim scales the generic GAIT 2392 model using the kinematic data to match the anthropometrics of the subject. Within OpenSim, there are two methods of scaling: 1. Manual and 2. Measurement based. Manual scaling uses segment lengths inputted by the user based off medical imaging information, such as CT scans or MRIs.

Measurement-based scaling uses the distances between the experimental markers measured during the collection of motion capture data and virtual markers on the OpenSim model. For this study, measurement-based scaling will be used.

The GAIT 2392 model represents a subject that is 1.8 meters in height and 75.16 kg in weight. For this study, this model was scaled down to a subject-specific model that is 5.35 kg in weight and 0.56 m in height. By using marker-based scaling, the virtual marker on the model was matched to the experimental anatomical marker placement (Figure 10), and the respective scale factors were calculated and applied (Table 1). The scaled model is then generated (Figure 11). These markers were also used to define the body segments of the model (Table 2).

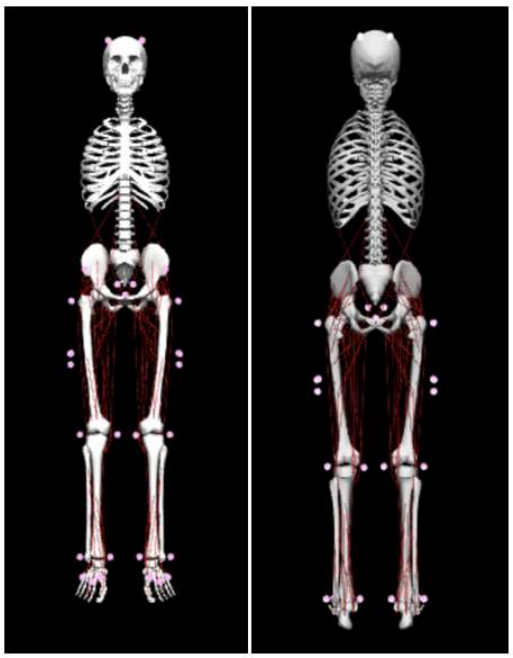

OpenSim Marker Model
1. Right and Left Head Posterior
2. Right and Left Head Anterior
3. Pelvis Cluster (1,2,3)
4. Right and Left Lateral Thigh Cluster (1,2,3)
5. Right and Left Lateral Knee
6. Right and Left Medial Knee
7. Right and Left Lateral Ankle
8. Right and Left Medial Ankle
9. Right and Left Lateral Foot
10. Right and Left Medial Foot
11. Right and Left Toe
12. Right and Left Trochanter
13. Right and Left ASIS

Figure 12. Custom marker model used in OpenSim. ASIS = Anterior Superior Iliac Spine.

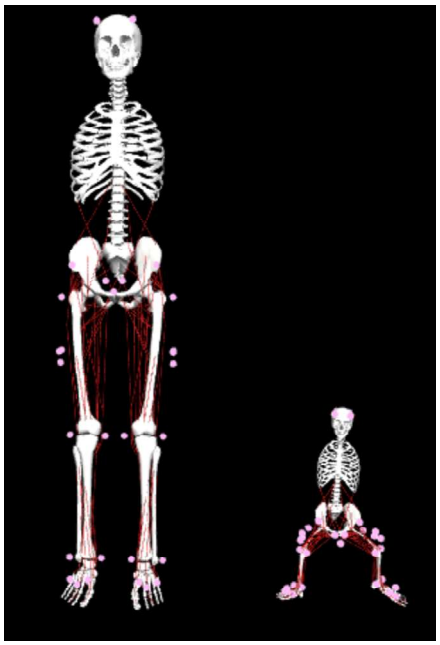

Figure 13. OpenSim subject-specific scaled infant model. Left: Adult and Right: Scaled Infant

Table 1. Scale factors of body to create subject-specific OpenSim model of infant.

Body Name	Measurement(s) Used	Applied Scale Factor(s)
Torso	Torso	0.428863
Pelvis	Pelvis	0.468240
R. and L. Femur	Thigh	0.219688
R. and L. Tibia	Shank	0.283175
R. and L. Talus	Foot	0.459718
R. and L. Calcaneus	Foot	0.459718
R. and L. Toes	Foot	0.219688

Table 2. Body segments and defining marker pairs.

Segment Name/Measurements	Marker Pairs			
Torso	R. Head Anterior	R. ASIS	L. Head Anterior	L. ASIS
Pelvis	R. ASIS		L. ASIS	
Thigh	R. ASIS	R. Lateral Knee	L. ASIS	L. Lateral Knee
Shank	R. Medial Knee	R. Medial Ankle	L. Medial Knee	L. Medial Ankle
Foot	R. Medial Ankle	R. Toe	L. Medial Ankle	L. Toe

These scale factors were compared to the average upper segment lower segment (USLS) ratio seen in infants. The average USLS ratio in infants is 1.7, where they compare the upper segment, consisting of the torso, and the lower segment, consisting of the legs [20]. The USLS ratio of the scaled subject-specific OpenSim infant model is 1.61, a 5% difference.

3.2 Inverse Kinematics

The inverse kinematics tool computes the joint angles by going through each time step (frame) of the motion recorded, and computes coordination values of the model that best represent the motion of the experimental model. It uses a weight least squares equation to minimize the marker and coordination errors (1).

$$\min_{q} = \left[\sum_{i \in markers} w_i \left\| x_i^{exp} - x_i(q) \right\|^2 + \sum_{\substack{j \in unprescribed \\ coord}} w_j (q_j^{exp} - q_j)^2\right] \quad (1)$$

Where:

q: vector of generalized coordinates being solved for

x_i^{exp}: experimental positions of marker i

$x_i(q)$: position of corresponding virtual marker

w_i: marker weights

q_j^{exp}: experimental value for coordinate j

w_j: coordinate weights

Experimental kinematic data is used as the input into the inverse kinematics tool for the model to match the virtual markers to the motion of the experimental tracking markers. A motion file of the joint coordinates (joint angles and translations) computed by the tool is given as an output file and will be used as the input to use in the inverse dynamics tool to calculate joint moments.

The infant participated in a 30-second positional task: lying in the supine position and allowed to move naturally and freely. No restrictions of motion were imposed on the infant at any position and was not specifically encouraged or discouraged to perform any specific movement.

3.3 Inverse Dynamics

Using the kinematics describing the movement of the model and a ground reaction force applied at the pelvis of the subject in the supine position, the inverse

dynamics tool in OpenSim can be used to calculate the generalized external net forces and torques at each joint during the movement. Inverse dynamics aims to solve the equation of motion (2) by using what can be found with the kinematic data to solve for the unknown forces and torques.

$$\tau = M(q)\ddot{q} + C(q, \dot{q}) + G(q) \quad (2)$$

Where:

$q, \dot{q}, \ddot{q}$: vectors of generalized positions, velocities, and accelerations, respectively

M: system mass matrix

C: vector of Coriolis and centrifugal forces

G: vector of gravitational forces

τ: vector of generalized forces and torques

It is important to remember the inverse dynamics tool does not consider muscle forces in calculating the external torque, as explained in section 2.2.3. For this reason, no muscle parameters of the adult male represented in the generic model were changed to that of an infant. Rather, the inverse dynamics tool uses the GRF and the respective moment arm from the location of the joint axis to calculate the external torques seen at the joint, as well as torques due to gravitational forces. For this study, a constant value of 52.48 N normal to the ground was placed on the pelvis to represent the infant's weight. The GRF as well as all moments of the force plate in all other directions were set to a value of 0 N.

Chapter IV

Results

Joint angles and moments obtained from the dynamic trial were applied to the subject-specific custom GAIT 2392 model. Direct comparisons of the data was made with relevant literature for model validation. A single kick was defined as a movement of the hip joint, beginning from an extended position, moving through a single flexion phase, and the returning to the extended position. Table 3 identifies the start of the kick at hip extension, to hip flexion, and then back to hip extension to end the kick in the time domain represented in seconds.

Table 3. Progression of kicking motion with corresponding time (s)

	Time (s)		
	Start (Extension)	Middle (Flexion)	End (Extension)
Right Hip	1.25	1.45	1.71
Left Hip	1.6	1.66	2

4.1 Hip Joint Range of Motion

The hip joint is the articulation between the femoral head and the acetabulum of the pelvis, flexion and extension occurring in the sagittal plane. The results show a minimum joint angle in the right hip of 22.2° and a maximum joint angle of 66.6° (Figure 13). A minimum joint angle of 23.2° and a maximum joint angle of 66.3° is observed in the left hip joint (Figure 14).

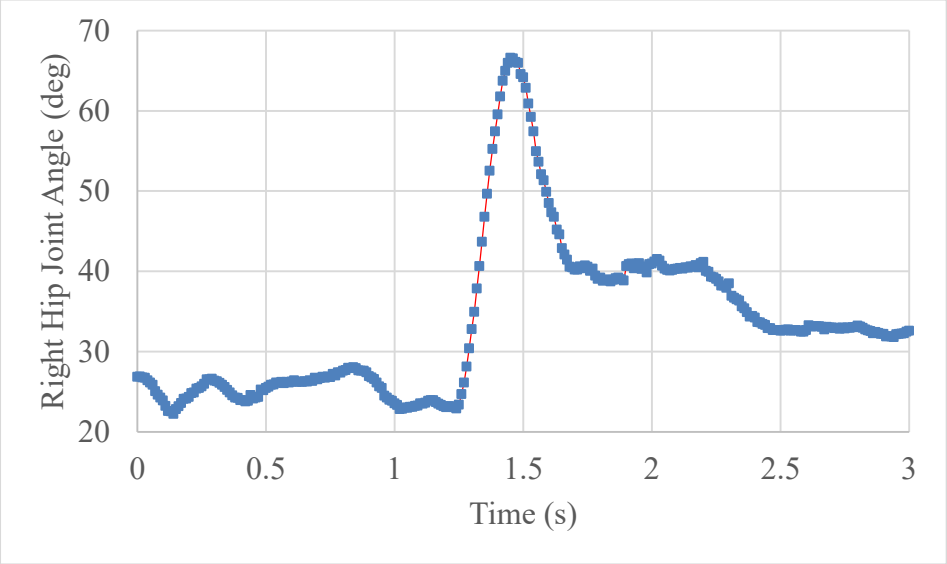

Figure 14. Right hip joint angle data exported through inverse kinematics tool on OpenSim.

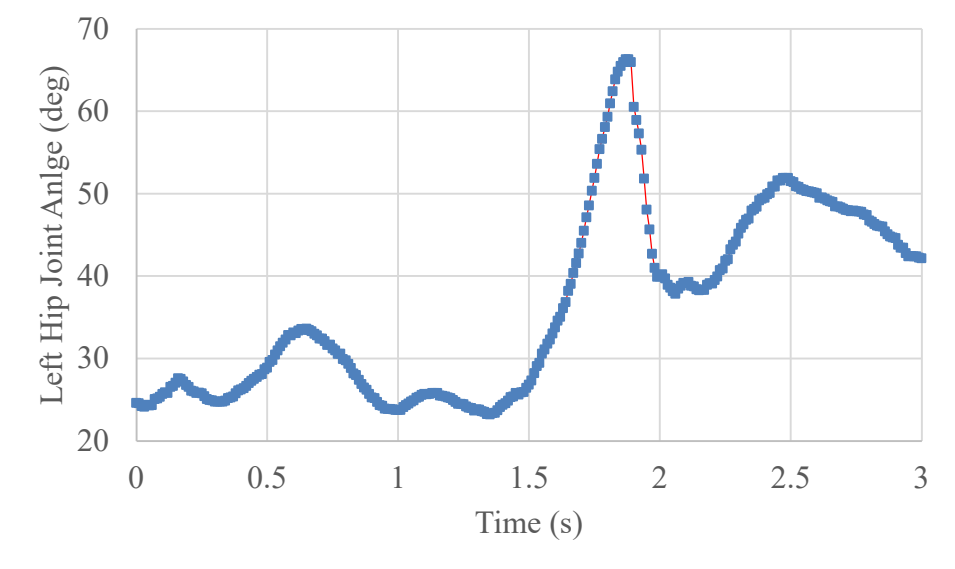

Figure 15. Left hip joint angle data exported through inverse kinematics tool on OpenSim.

As seen in Figure 13 and 14, the previously characterized kick is observed in the time(s) listed in Table 3 as a peak in the data. The hip joint results of the specified kick and its corresponding time(s), seen in Table 3, are plotted (Figure 15 and 16).

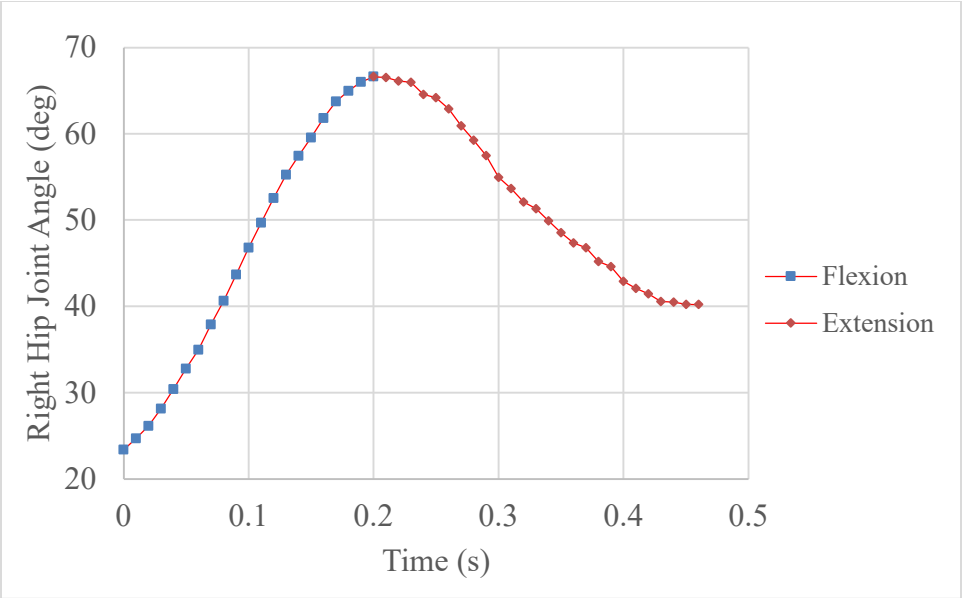

Figure 16. Right hip joint angle data during kick (isolated) exported through inverse kinematics tool on OpenSim.

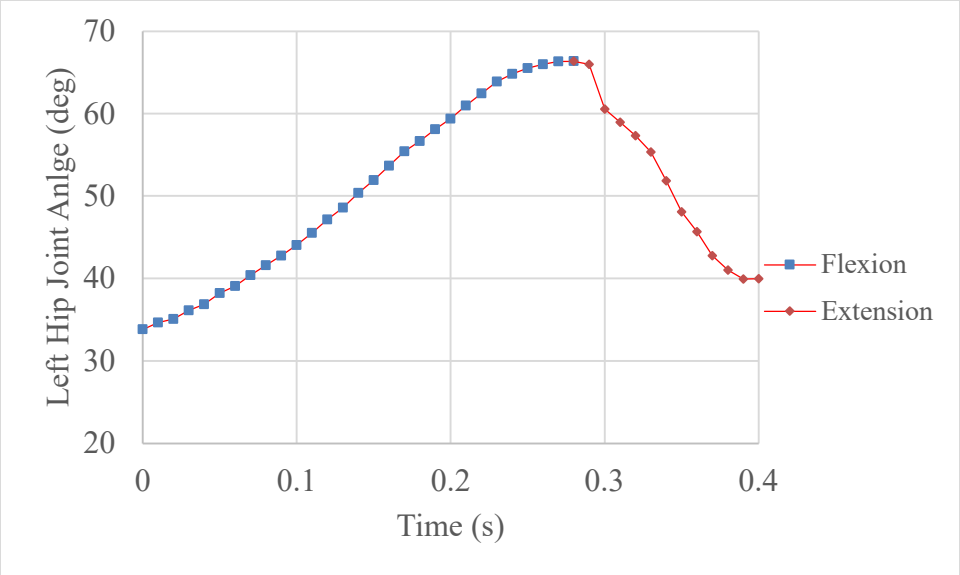

Figure 17. Left hip joint angle data during kick (isolated) exported through inverse kinematics tool on OpenSim.

4.2 External Hip Joint Moment

The generalized external net torques are determined through the inverse dynamics tool in OpenSim. The external joint moments for the hip joint are shown in figures 18 and 19.

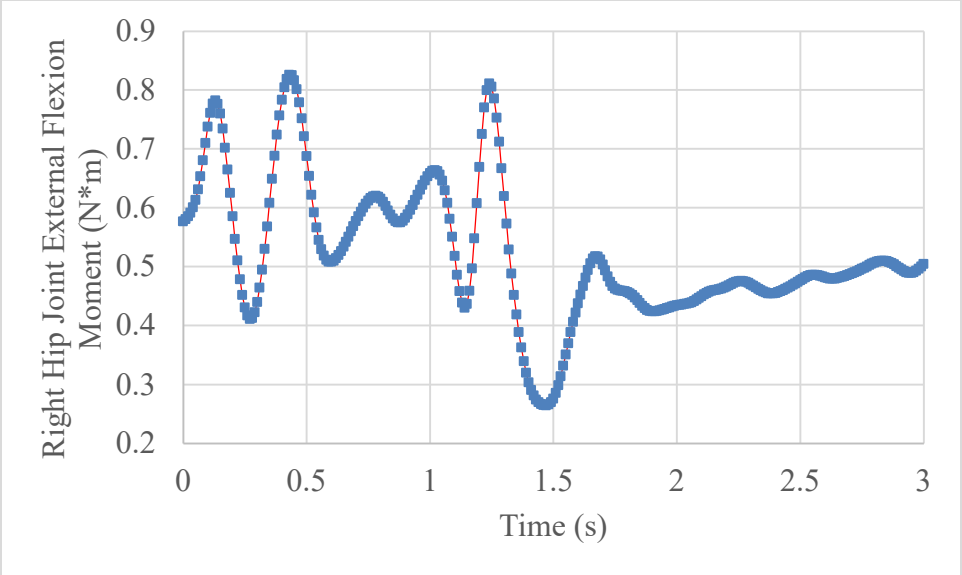

Figure 18. External right hip joint moment data exported through inverse dynamics tool on OpenSim.

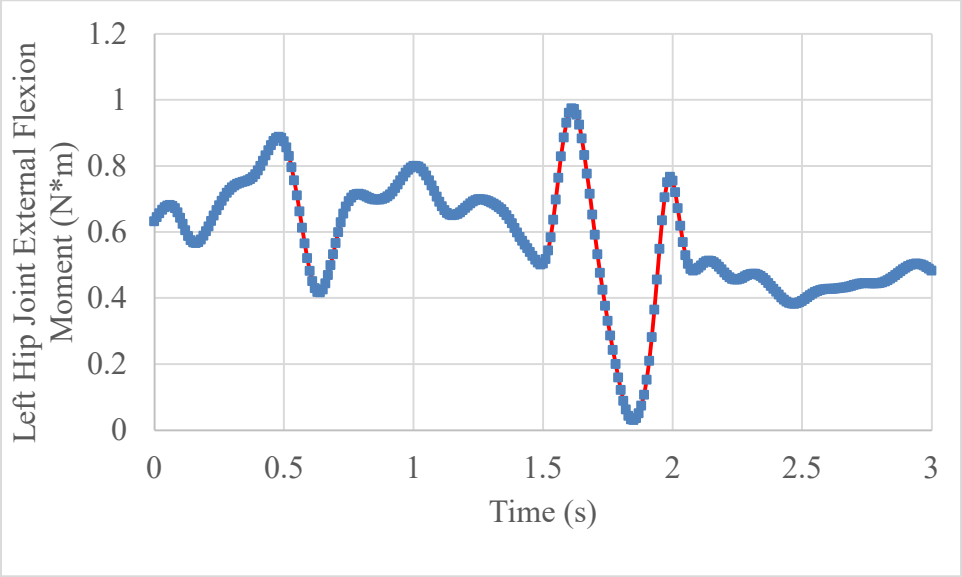

Figure 19. External left hip joint moment data exported through inverse dynamics tool on OpenSim.

As seen in Figure 18 and 19, the previously characterized kick is observed in the time(s) listed in Table 3 as a peak in the data. The external hip joint moment results of the specified kick and its corresponding time(s) for the right and left hip joint, seen in Table 3, are plotted (Figure 20 and 21).

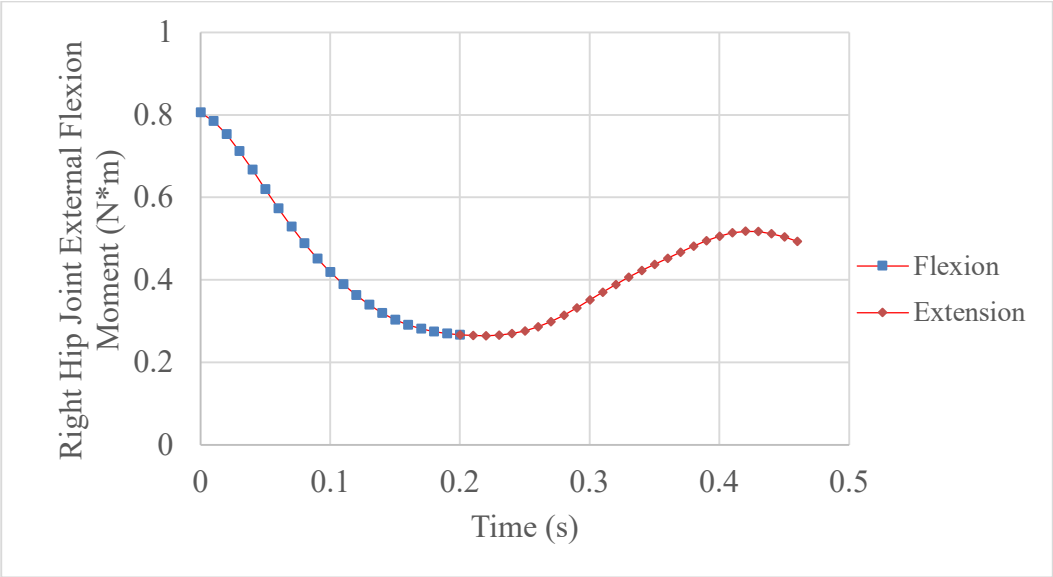

Figure 20. External right hip joint moment during kick (isolated) data exported through inverse dynamics took on OpenSim.

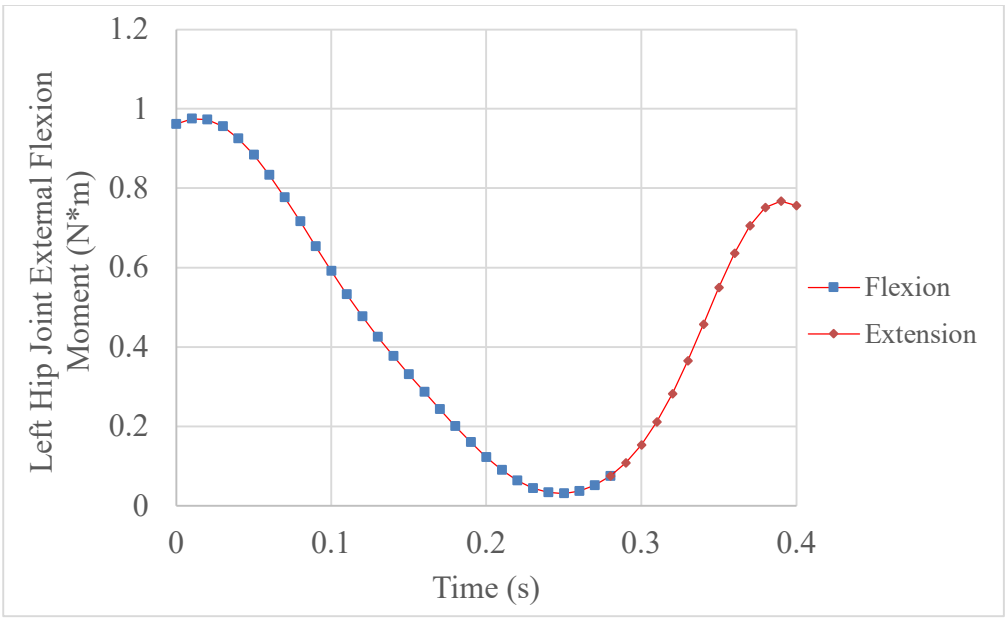

Figure 21. External left hip joint moment during kick (isolated) data exported through inverse dynamics tool on OpenSim.

4.2.1 Ground Reaction Force Validation

Compared to Schneider et al. (1990)'s net joint torque calculations, OpenSim's inverse dynamics tool considers the gravitational and interactive torques, explained in section 2.2.3. Because the torque caused by muscle forces is not considered, the external moment at a joint calculated by OpenSim is dependent on the weight of the infant, as well as the ground reaction force data used as an input to run inverse dynamics rather than any muscle parameters. This is seen in the plotting of the external joint moment with an increase in weight and respective ground reaction force value. The same trend of external hip joint moment is observed, while the values are changed by the same scale factor of weight difference. A scale factor of 11.96 was applied to the weight during the scaling and inverse dynamics steps to represent a difference in weight of the infant subject (5.35 kg) and an adult woman (64 kg) (Figure 22 and 23).

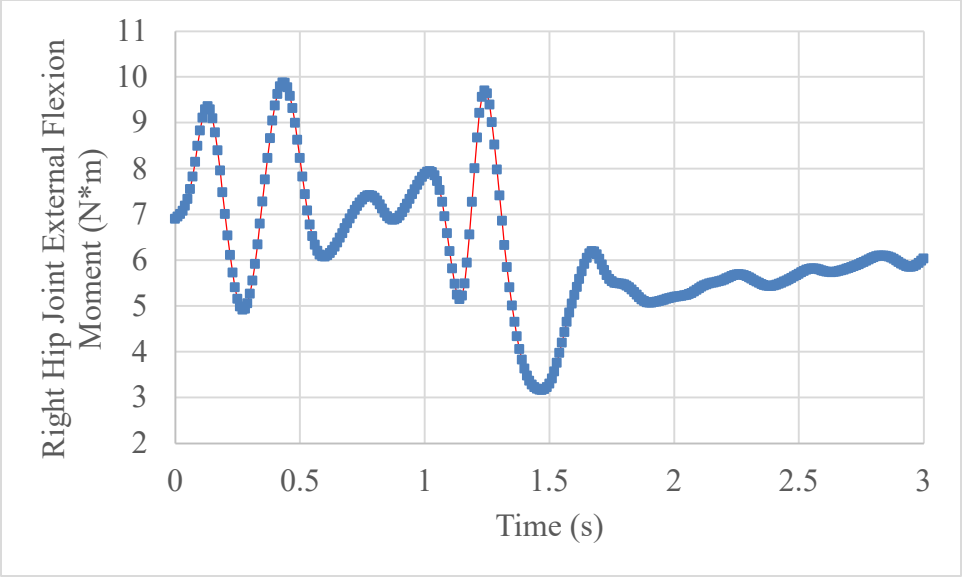

Figure 22. External right hip joint moment data exported through inverse dynamics tool on OpenSim. The weight of the subject was changed by a scale factor of 11.96 compared to the weight used to model the infant subject.

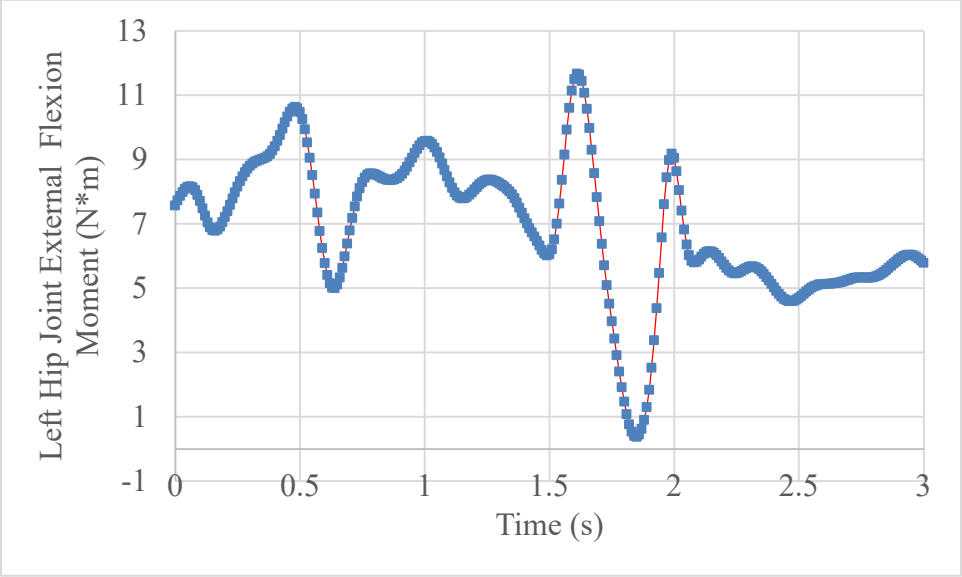

Figure 23. External left hip joint moment data exported through inverse dynamics tool on OpenSim. The weight of the subject was changed by a scale factor of 11.96 compared to the weight used to model the infant subject.

When the external hip joint moment data of a subject with an increased weight (64 kg) (Figure 22 and 23) is compared to that of the original infant (5.35 kg) (Figure 18 and 19), the same trendline is observed, with the values of the joint moment increased by the same scale factor applied to the weight (11.96). This validates the inverse dynamics tool on OpenSim uses the gravitational and interactive torques to calculate external joint moments.

Chapter V

Discussion, Limitations, Future Works, and Conclusion

The purpose of this study was to create a preliminary musculoskeletal computational model of an infant to study the biomechanics of the lower extremity. By using motion-capture data and the ground reaction force value representing the infant weight, a model was created using OpenSim. Based on the results presented in Chapter 4, the preliminary results show the infant musculoskeletal model that was developed will properly portray the biomechanics behind infant movement, and can quantify joint angle and external moment to further study pathologies in infants.

5.1 Discussion

5.1.1 Analysis of Joint Angle

A spontaneous kick movement is categorized as the hip joint starting at the extended position, moves through a flexed stage, and moves back to the extended position. The results of hip joint angle produced through OpenSim can be compared to that of Schneider et al.'s (1990) research in joint angle (Figure 24).

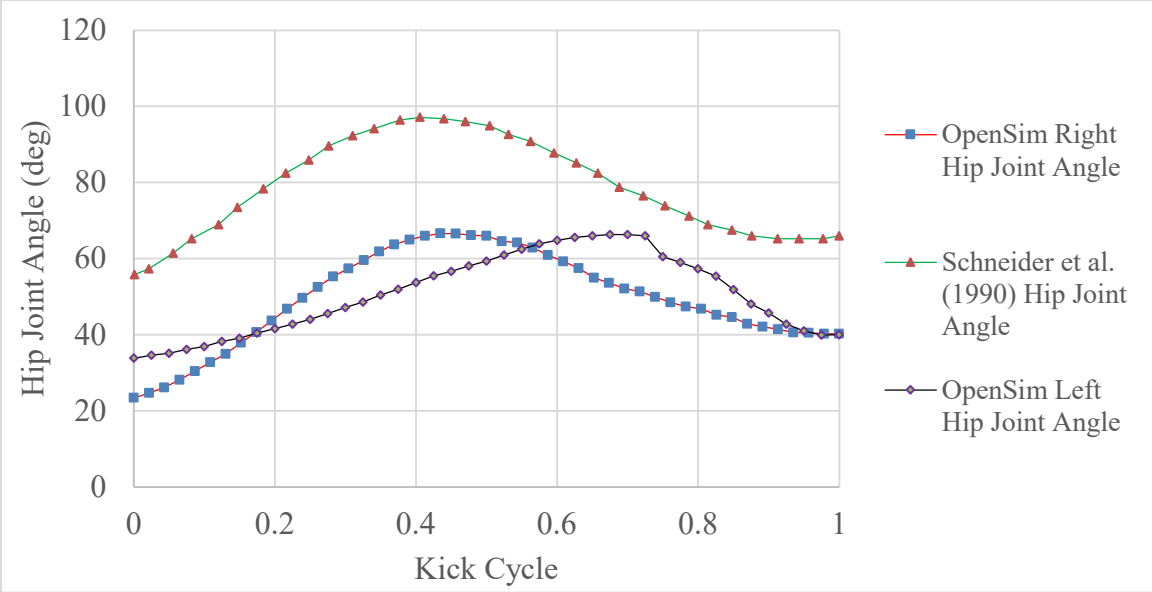

Figure 24. Hip joint angle comparison between OpenSim's results and Schneider et al.'s (1990) data.

As explained in Table 3, the kicking movement observed in the experimental data used in OpenSim's inverse kinematics tool occurs within a smaller time frame compared to the data seen in literature (Right hip: 0.4 s, Left hip: 0.46 s, Literature: 0.8 s). When observing the trend, however, a similar slope is noticeable as the hip enters the kicking motion. There is a maximum difference of 30.5° and 30.8° is observed in the right and left hip joint angle, respectively, compared to that found in literature. This maximum difference was observed at the corresponding time of maximum hip flexion angle. This difference, however, can be explained by a major difference in data collection methods. In the methods used by Schneider et al. (1990), the infant subject's upper extremity was immobilized while the lower extremity could move freely and naturally. In the data collected for this study, however, there were no movement restrictions placed on the

infant. Both the upper extremity as well as the lower extremity could move freely and naturally, limiting the sole focused movement of the lower extremity.

5.1.2 Analysis of Joint Moment

The hip joint moment data obtained through OpenSim was also compared to the data found in literature. In both results, an increase in moment is observed during the flexion, and a decrease in moment during the extension of the hip (Figure 25).

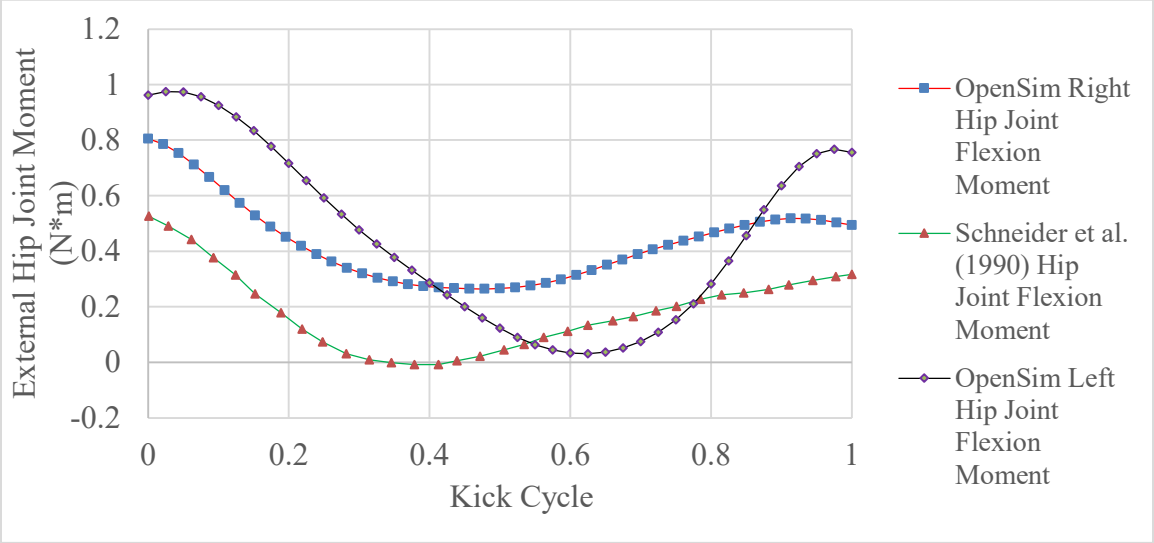

Figure 25. External hip joint moment comparison between OpenSim's results and Schneider et al.'s (1990) data.

Like the results comparison of the hip joint angle, a similar trend is observed between hip joint moment results produced through OpenSim and that found in literature. A difference of 0.275 N*m and 0.0827 N*m was observed, in the right and left hip joint respectively, at the point of maximum hip flexion angle. This difference in moment can be attributed to not only the upper extremity being able to move freely but also the

difference in kicks the infant in each study performs. Due to the limitation of accessible data, and the fact that infant subjects are unable to control their movements, recreating specific kicking motions is nearly impossible. The similarity in how the external joint moment behaves with respect to hip joint flexion and extension is observed in both the results of this study, and results found in literature. As seen in figures 20 and 21, the external hip joint moment for both the right and left hip decreases as the hip joint undergoes flexion, and then increases as the hip returns to the extended position. This trend coincides with the results found in Schneider et al.'s (1990) study in their joint moment calculations.

5.2 Limitations

Although this study can be considered successful, there were however a few limitations that comes with the results. The limits affecting the current study are listed below.

As mentioned in chapter one, an infant as a subject of a study that is movement based is a big limitation, to not only this study but any future studies. Infants in the developmental stage have no control of their movements, rather their movements are sporadic and more reaction-based than skill-based. This coupled with an infant's inability to listen to directions causes any recreating of specific movements impossible. This limits any direct comparison between previous studies found in literature and any new studies. Furthermore, the motion-capture data and kinetic data used in this study was recorded at the University of Arkansas Medical Center. Access to infants to be subjects to this study

was limited, and data could not be recollected throughout the study to get information needed.

During the data collection, specific segment anthropometric measurements were not recorded. These measurements are often used to validate the scaled model. For this study, however, the USLS segment ratio was used as the validation method, rather than a direct comparison to anthropometric measurements. Furthermore, only motion capture data was recorded on the single subject infant without any information of ground reaction forces corresponding to the movement. For this study, a constant value representing the weight of the infant was placed in the upward direction, while forces in all other directions were set to a value of 0. This is inaccurate as there are shear forces observed during the movement of the infant. Since inverse dynamics uses ground reaction force data to calculate joint moments, having the appropriate force plate data corresponding to the movement of the infant will produce more accurate data.

Since there is very limited information on infant movements and joint mechanics, validation of such a model becomes difficult. Schneider et al.'s (1990) research is, to the best of the researcher's knowledge, the only published study that provides information on joint mechanics to be used to compare any results obtained through OpenSim.

5.3 Conclusion

Based on the trends in hip joint angle and joint moments observed from this study and how it compares to that found in literature, it can be concluded this study was successful in the development of a preliminary computational infant musculoskeletal model with the data that was accessible. Despite each kick being spontaneous and

random, with varying hip joint angles and its corresponding moments, the trend of the hip joint angle and external hip joint moment of the results is comparable to that of Schneider et al. (1990). This model is the first step to creating a complete model of infant biomechanics for further analysis of how certain pathologies affect an infant's movement. Future studies like this are presented in section 5.4.

5.4 Future Work

Based on the results, future studies should include applying the current methodology in developing a computational infant musculoskeletal model by collecting more complete motion-capture and force plate data. This would allow for a better understanding of the joint angles and moments. Furthermore, applying the same methodology as found in Schneider et al.'s (1990) research could be beneficial as it would be a direct comparison to previously published results on infant biomechanics. Future studies should also include applying the same methodology to a larger population. This would allow for a comparison of results between infants of different size, weight, and age, providing a better understanding of the biomechanics of infants. This will also minimize any anomalies associated with subject-specific testing.

Another future step that needs to be taken is applying the static optimization tool on OpenSim. This tool is an extension of the inverse dynamics tool, which further computes individual muscle forces from general forces by taking into account muscle parameters of the model, such as maximum isometric force, optimal fiber length, tendon slack length, and pennation angle. By changing these muscle parameters, a fully scaled infant musculoskeletal model will be developed, and will allow for the calculation of

internal joint moments and specific muscle forces that are required to perform movements, which can be vital in understanding the biomechanics of infant movement in both healthy and pathologically affected infants.

References

[1] Matsuo, T., Fleisig, G.S., Zheng, N., Andrews, J.R., 2006. "Influence of shoulder abduction and lateral trunk tilt on peak elbow varus torque for college baseball pitchers during simulated pitching" J. Appl. Biomech.

[2] Anderson, A.E., 2019. "CORR Insights®: Patient Age and Hip Morphology Alter Joint Mechanics in Computational Models of Patients with Hip Dysplasia." Clin. Orthop. Relat. Res. 477, 1246–1248.

[3] Dao, T.T., Marin, F., Pouletaut, P., Charleux, F., Aufaure, P., Ho Ba Tho, M.C., 2012. "Estimation of accuracy of patient-specific musculoskeletal modelling: Case study on a post polio residual paralysis subject." Comput. Methods Biomech. Biomed. Engin. 15, 745–751.

[4] Marra, M.A., Vanheule, V., Rene, F., Koopman, B.H.F.J.M., Rasmussen, J., Verdonschot, N., Andersen, M.S., 2015. "A subject-specific musculoskeletal modeling framework to predict in vivo mechanics of total knee arthroplasty." J. Biomech. Eng. 137, 020904.

[5] Rahman, M., Cil, A., Bogener, J., Stylianou, A., 2016. "Lateral collateral ligament deficiency of the elbow joint: A modeling approach". J. Orthop. Res. 1–11.

[6] Alizadeh, M., Knapik, G.G., Mageswaran, P., Mendel, E., Bourekas, E., Marras, W.S., 2020. "Biomechanical musculoskeletal models of the cervical spine: A systematic literature review." Clin. Biomech. 71, 115–124.

[7] Ghezelbash, F., Shirazi-Adl, A., Arjmand, N., El-Ouaaid, Z., Plamondon, A., 2016. Subject-specific biomechanics of trunk: musculoskeletal scaling, internal loads and intradiscal pressure estimation. Biomech. Model. Mechanobiol. 15, 1699–1712.

[8] Rasmussen, J., Tørholm, S., de Zee, M., 2009. “Computational analysis of the influence of seat pan inclination and friction on muscle activity and spinal joint forces.” Int. J. Ind. Ergon. 39, 52–57.

[9] Price, C., Morrison, S.C., Hashmi, F., Phethean, J., Nester, C., 2018. “Biomechanics of the infant foot during the transition to independent walking: A narrative review.” Gait Posture 59, 140–146.

[10] Anderson, V., Spencer-Smith, M., Wood, A., 2011. “Do children really recover better? Neurobehavioral plasticity after early brain insult.” Brain 134, 2197-2221.

[11] Guttmann, K., Flibotte, J., DeMauro, SB., 2018. “Parental perspectives on diagnosis and prognosis of neonatal intensive care unit graduates with cerebral palsy.” Journal of Pediatrics 203, 156-162.

[12] Baird, G., McConachie, H., Scrutton, D., 2000. “Parents’ perceptions of disclosure of the diagnosis of cerebral palsy.” Archies of Disease in Childhood 83, 475-480.

[13] Thelen, D.G., 2003. “Adjustment of muscle mechanics model parameters to simulate dynamic contractions in older adults.” Journal of Biomechanical Engineering 125(1), 70-77.

[14] Seow, C.Y., 2013. “Hill’s equation of muscle performance and its hidden insight on molecular mechanisms.” The Journal of General Physiology 142, 561-573.

[15] Dezateux, C., Rosendahl, K., 2007. “Developmental dysplasia of the hip.” Lancet 369, 1541-1552.

[16] USPTF, 2006. “Screening for developmental dysplasia of the hip: recommendation statement.” American Family Physician 73, 1992-1996.

[17] Bialik, V., Bialik, G.M., Blazer, S., Sujov, P., Wiener, F., Berant, M., 1999. "Developmental dysplsia of the hip: a new approach to incidence." Pediatrics 103, 93-99.

[18] Narayanan, U., Mulpuri, K., Sankar, W.N., Clarke, N.M., Hosalkar, H., Price, C.T., International Hip Dysplasia Institute, 2015. "Reliability of a new radiographic classification for developmental dysplasia of the hip." Journal of Pediatric Orthopedics 35, 478-484.

[19] Schneider, K., Zernicke, R.F., Ulrich, B.D., Jensen, J.L., Thelen, E., 1990. "Understanding movement control in infants through the analysis of limb intersegmental dynamics." Journal of Motor Behavior 22, 493-520.

[20] Kliegman, R.M., Jenson, H.B., Behrman, R.E., Stanton, B.F., 2007. "Nelson Textbook of Pediatrics 18th edition. Philadelphia: Saunders".

Appendix A

Tables

Table 4. Scale factors of body to create subject-specific OpenSim model of infant.

Body Name	Measurement(s) Used	Applied Scale Factor(s)
Torso	Torso	0.428863
Pelvis	Pelvis	0.468240
R. and L. Femur	Thigh	0.219688
R. and L. Tibia	Shank	0.283175
R. and L. Talus	Foot	0.459718
R. and L. Calcaneus	Foot	0.459718
R. and L. Toes	Foot	0.219688

Table 5. Body segments and defining marker pairs.

Segment Name/Measurements	Marker Pairs			
Torso	R. Head Anterior	R. ASIS	L. Head Anterior	L. ASIS
Pelvis	R. ASIS		L. ASIS	
Thigh	R. ASIS	R. Lateral Knee	L. ASIS	L. Lateral Knee
Shank	R. Medial Knee	R. Medial Ankle	L. Medial Knee	L. Medial Ankle
Foot	R. Medial Ankle	R. Toe	L. Medial Ankle	L. Toe

Table 6. Progression of kicking motion with corresponding time (s)

	Time (s)		
	Start (Extension)	Middle (Flexion)	End (Extension)
Right Hip	1.25	1.45	1.71
Left Hip	1.6	1.66	2

Appendix B

Figures

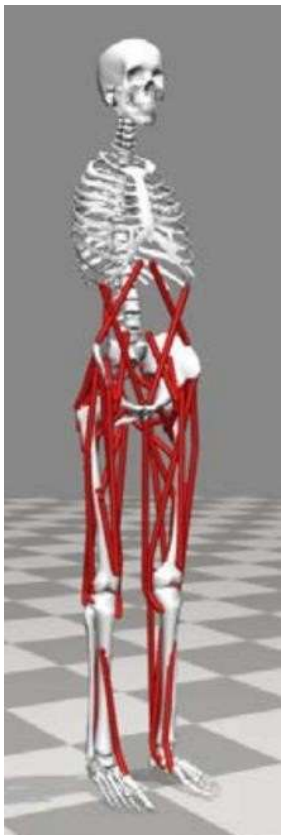

Figure 26. OpenSim Gait 2392 Model

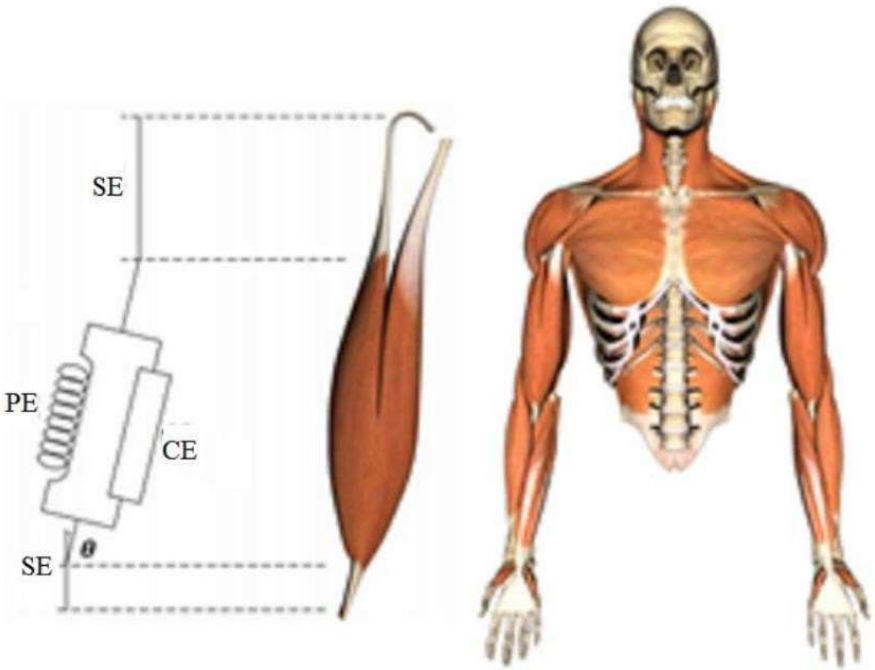

Figure 27. Hill Model used in OpenSim models. CE predicts active muscle forces, PE predicts elastic and passive muscle force, and SE predicts the overall summation of CE and PE forces.

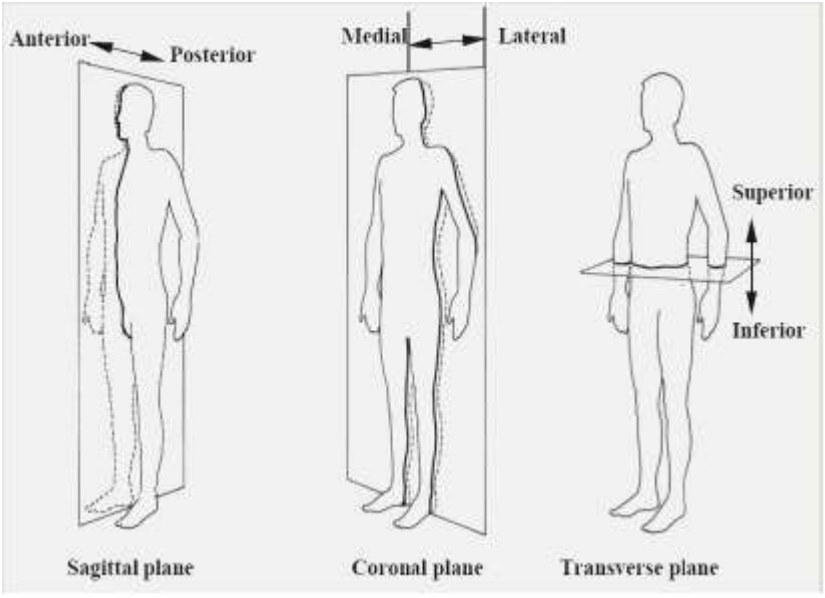

Figure 28. Plane of movements: sagittal, coronal, and transverse planes [2].

Figure 29. Anatomy of the hip joint: A. Femoral Head and B. Acetabulum.

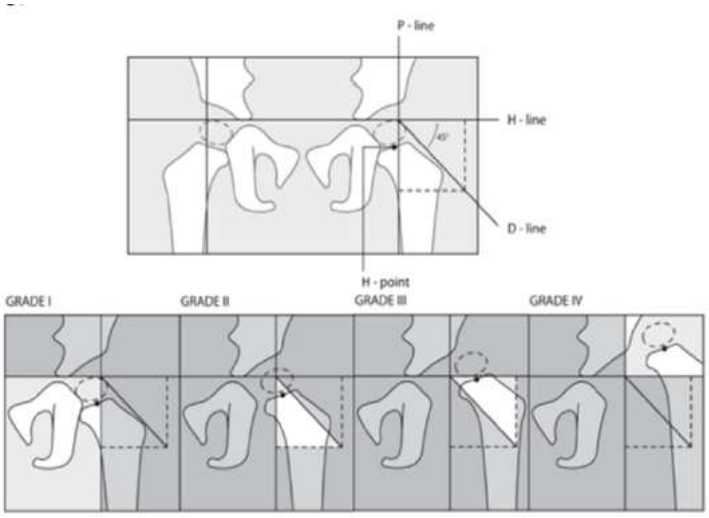

Figure 30. Classification of developmental dysplasia of the hip. Grade 1 being the mildest and Grade 4 being the most extreme. Grade I: The H-point is medial to the P-line. Grade II: The H-point is lateral to the P-line and at/medial to the D-line. Grade III: The H-point is lateral to the D-line and at/inferior to the H-line. Grade IV: The H-point is superior to the H-line.